Single order soft X-ray diffraction with quasi-random radius pinhole array spectroscopic photon sieves*

Zhang Qiang-Qiang(张强强), Wei Lai(魏 来), Yang Zu-Hua(杨祖华), Qian Feng(钱 凤), Fan Quan-Ping(范全平), Zhang Bo(张 博), Gu Yu-Qiu(谷渝秋), and Cao Lei-Feng(曹磊峰)†

Research Center of Laser Fusion, China Academy of Engineering Physics, Mianyang 621900, *China*

(Received 15 August 2013; revised manuscript received 9 September 2013; published online 20 February 2014)

A novel single order diffraction grating in the soft X-ray region, called quasi-random radius pinhole array spectroscopic photon sieves (QRSPS), is proposed in this paper. This new grating is composed of pinholes on a substrate, whose radii are quasi-random, while their centers are regular. Analysis proves that its transmittance function across the grating bar is similar to that of sinusoidal transmission gratings. Simulation results show that the QRSPS can suppress higher-order diffraction effectively. And the QRSPS would still retain its characteristic of single order diffraction when we take the effect of X-ray penetration into account. These properties indicate that the QRSPS can be used in the soft X-ray spectra measurement.

Keywords: diffraction properties, diffraction gratings, soft X-rays, single-order diffraction

PACS: 42.79.Dj, 42.25.Fx, 42.62.Fi **DOI:** 10.1088/1674-1056/23/4/044215

1. Introduction

The measurement of soft X-ray spectra plays an important role in studying inertial confinement fusion.[1] As an old optics device, transmission grating is widely used in soft X-ray diagnoses.[2–4] As is well known, classical black–white transmission gratings (TGs) have multi-order diffractions.[5] Owing to the overlap of higher-order diffractions, soft X-ray spectra obtained from the 1st order diffraction will be contaminated, and thus limit the precision of the soft X-ray spectra measurement.

Ideal sinusoidal transmission grating (STG) only has 0th and $\pm$1st order diffractions since its transmittance function is a sinusoidal function.[6] However, the STGs cannot be used in the X-ray region because of an associated phase problem, which reintroduces higher-order diffraction.[4] In 2001, Kipp *et al.*[7] proposed the concept of photon sieves in the design of a binary Fresnel zone plate. Much theoretical and experimental studies related to photon sieves have been reported recently, such as spiral photon sieves,[8] compound photon sieves,[9] and differential-interference-contrast imaging using modified photon sieves.[10] An innovative method, namely binary sinusoidal transmission grating which can suppress higher-order diffractions, was proposed by Cao *et al.*[11] in 2007. In this concept, the transmission is a two-dimensional (2D) distribution step function and only takes binary values of 0 and 1. Based on this theory, some binary single order diffraction gratings have been developed.[12–21] A quantum-dot-array diffraction grating (QDADG) has been reported by Wang *et al.*,[12,13] and in its design a great many quantum dots are distributed on a substrate, which obey the sinusoidal function. A QDADG for visible light has been fabricated and the experiment has shown that higher-order diffractions disappear as predicted. Kuang *et al.*[15] reported on a different way to realize sinusoidal transmission function, namely QSTG, the designed transmittance function is very close to that of an ideal STG. The shortages of QDADG and QSTG are that each of them needs an underlayment since they do not stand themselves, while most underlayment absorbs X-ray seriously. Zang *et al.*[17,18] presented a zigzag transmission grating composed of a series of zigzag-profiled strips, which can also achieve the purpose of single order diffraction. But the zigzag-profiled strips demand an extremely critical nanofabrication technique. Recently, Wei *et al.*[19] and Cao *et al.*,[20,21] developed a new single order diffraction grating called the spectroscopic photon sieve (SPS), which suppresses higher-order diffractions and stands freely by distributing numbers of randomly positioned pinholes with an equal radius on an aurum substrate.

In this paper, a new single order soft X-ray diffraction optical device called quasi-random radius pinhole array spectroscopic photon sieves (QRSPS) is proposed. We deduce the transmittance function of the QRSPS across the grating bar and the result is similar to that from sinusoidal transmission grating. Simulations prove that the QRSPS suppresses higher-order diffractions effectively. The QRSPS would retain its excellent characteristics when X-ray penetration is included. Compared with SPS mentioned above, the QRSPS has regular pinhole positions and is therefore easier to fabricate.

2. Design of QRSPS

The newly designed QRSPS is composed of quasi-random radius pinholes as shown in Fig. 1. The basic unit is a $d \times d$ square, inside which there are many pinholes. The radii

*Project supported by the National Key Scientific Instruments and Equipments Development of Special Item, China (Grant No. 2012YQ130125) and the National Natural Science Foundation of China (Grant No. 11375160).

†Corresponding author. E-mail: liaode_2002@yahoo.com.cn

© 2014 Chinese Physical Society and IOP Publishing Ltd

of the pinholes are evenly quasi-random in a range of $[0, d/2]$, while its origin is fixed at the center of the square. The pinholes are transparent for incident light while the rest is opaque. This pattern is free-standing without underlayment. Considering gold high absorption of X-ray, we select gold foil as the material of our new grating (black in Fig. 1). To fabricate such a grating with 1000 line/mm, we use the technology of electron-beam lithography and X-ray lithography. Compared with the spectroscopic photon sieve mentioned in Refs. [19]–[21], the QRSPS is easy to fabricate due to its regular pinhole positions.

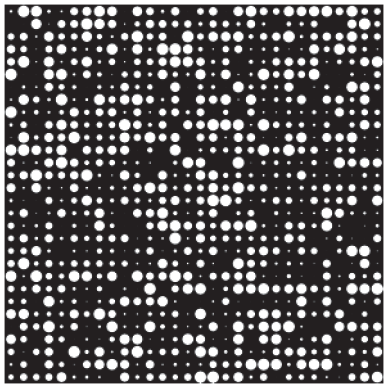


Fig. 1. Designed pattern of the QRSPS (30×30 units).

The transmittance function of the QRSPS is

$$t(x,y) = \begin{cases} 1, & (x,y) \in \text{ pinhole}, \\ 0, & (x,y) \notin \text{ pinhole}. \end{cases} \tag{1}$$

Suppose that there are n basic units along the vertical axis, then $t(x)$ can be expressed as the ratio of the total transparent length along the vertical axis at coordinate x to the whole length nd as follows:

$$t(x) = \int t(x,y)\,\mathrm{d}y = \lim_{n\to\infty} \frac{\sum_i 2\sqrt{r_i^2 - (x-d/2)^2}}{nd}, \tag{2}$$

where r_i is the radius of the i-th pinhole along the vertical axis. The probability density function of pinhole radius r is

$$P(r) = \frac{1}{d/2-0} = \frac{2}{d}, \quad r \in [0, d/2]. \tag{3}$$

Rank r as r_j according to the value, and $\Delta r_j = r_j - r_{j-1}$. Hence $t(x)$ can be simplified into

$$\begin{aligned} t(x) &= \lim_{n\to\infty} \frac{\sum_j 2\sqrt{r_j^2 - (x-d/2)^2} \cdot nP(r_j)\Delta r_j}{nd} \\ &= \lim_{n\to\infty} \frac{\sum_j 4\sqrt{r_j^2 - (x-d/2)^2}}{d^2} \Delta r_j \\ &= \frac{4}{d^2} \int \sqrt{r^2 - (x-d/2)^2}\,\mathrm{d}r, \end{aligned} \tag{4}$$

where $\mathrm{d}r$ denotes the average distance of r when n is large enough. The interval of integral is $[d/2 - x \cdot d/2]$ when $x \in [0, d/2]$, and is $[x - d/2, d/2]$ when $x \in [d/2 \cdot d]$. Finally we obtain

$$\begin{aligned} t(x) = &\sqrt{\frac{1}{4} - \left(\frac{x}{d} - \frac{1}{2}\right)^2} - 2\left(\frac{x}{d} - \frac{1}{2}\right)^2 \\ &\times \ln\left|\frac{1}{2} + \sqrt{\frac{1}{4} - \left(\frac{x}{d} - \frac{1}{2}\right)^2}\right| \\ &+ 2\left(\frac{x}{d} - \frac{1}{2}\right)^2 \ln\left|\frac{x}{d} - \frac{1}{2}\right|. \end{aligned} \tag{5}$$

It is obviously symmetrical as shown and compared with the transmittance function of STG (half of it is shown here for convenience) in Fig. 2. We can see that those two curves are analogous to each other. Therefore we can expect that the QRSPS and STG should have very similar diffraction properties. Furthermore, as a result of the symmetry of the design of the QRSPS, the transmittance function along the vertical axis $t(y)$ should have the same expression as $t(x)$, and the diffraction pattern of the QRSPS should also have symmetry along the horizontal and the vertical axes.

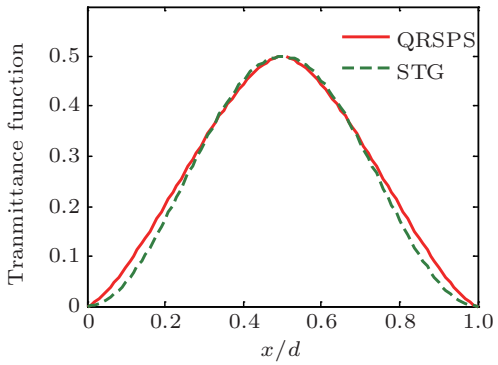


Fig. 2. (color online) Transmittance functions of the QRSPS and the STG.

3. Simulation of diffraction properties

3.1. Diffraction patterns of the STG and the QRSPS

To validate the design, we simulate the diffraction processes of sinusoidal transmission grating, the QRSPS and classical black–white transmission grating (1:1). Parameters used in the simulations are listed in Table 1.

Table 1. Parameters used in the simulation.

Wavelength λ/nm	Period of grating d/μm	Diffraction distance Z/m	Grating array /μm^2
0.3	1.0	0.6625	30×30

Suppose a plane wave of wavelength λ and amplitude A_0 incident normally on a grating. According to the diffraction theory of Kirchhoff, the diffraction pattern is

$$U(\xi,\eta) = \frac{1}{\mathrm{i}\lambda} \iint_{\Sigma} A_0 t(x,y) \frac{\mathrm{e}^{\mathrm{i}kR}}{R} \cdot \frac{1}{2}(1+\cos\theta)\,\mathrm{d}x\,\mathrm{d}y, \tag{6}$$

where the wave number $k = 2\pi/\lambda$, $\cos\theta = Z/R$, and R is the distance between point (x, y) and point (ξ, η).

The distribution of the diffraction field of classical black–white transmission grating is illustrated in Fig. 3(a). As expected, classical black–white transmission grating has multi-order diffractions. The STG has a diffraction pattern of single order, which is shown in Fig. 3(b).

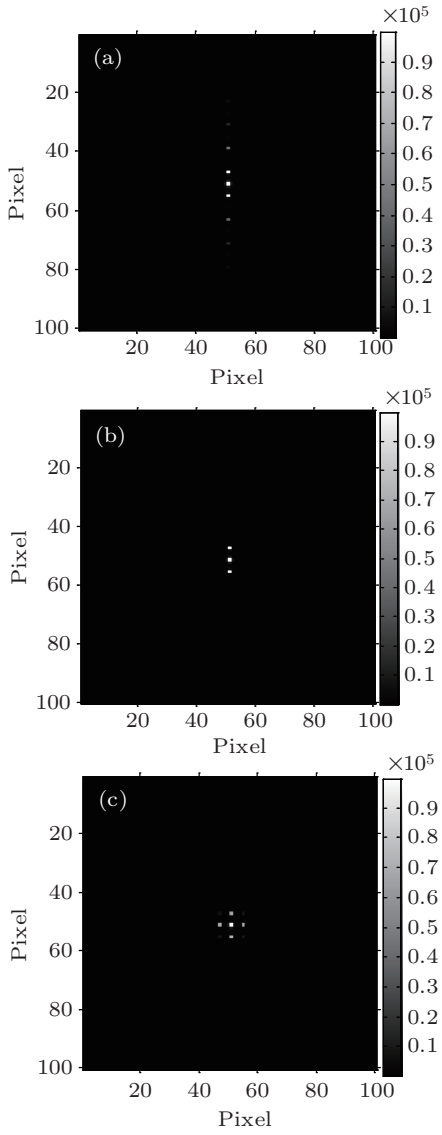


Fig. 3. Simulation results for (a) diffraction pattern of classical black–white transmission grating (1:1), (b) diffraction pattern of STG, and (c) diffraction pattern of QRSPS.

Figure 3(c) shows the diffraction pattern of the QRSPS, which has nine light spots. The 0th order is the brightest in the middle, while the 1st order is the four light spots around the 0th order. There are also four weaker spots at the four corners. But along the horizontal axis or the vertical axis there are only the 0th order and the $\pm$1st order, while other orders are strongly suppressed. What is more, the diffraction pattern of the QRSPS is symmetric around the horizontal and the vertical axes as expected.

The above results are also proved by a 1D diffraction pattern of those gratings as shown in Fig. 4. The 0th and $\pm$1st orders of the QRSPS are head and shoulders above the QRSPS's higher-order diffraction, respectively. In fact, the intensity of the 1st order is over 300 times higher than that of the 3rd order. Hence, we can conclude that the QRSPS suppresses higher-order diffraction effectively.

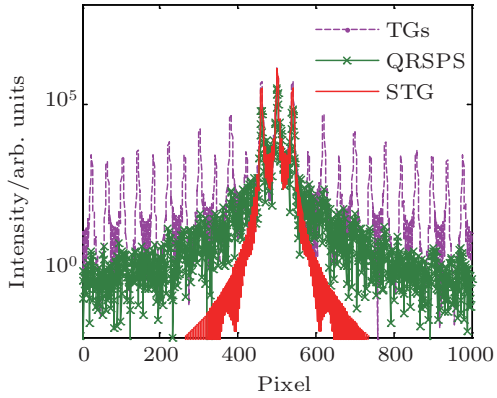


Fig. 4. (color online) 1D diffraction pattern of the classical black–white transmission grating (TG) and the QRSPS.

3.2. Diffraction properties of the QRSPS for different wavelengths

We have also numerically calculated the diffraction patterns of the QRSPS at different incident wavelengths. The

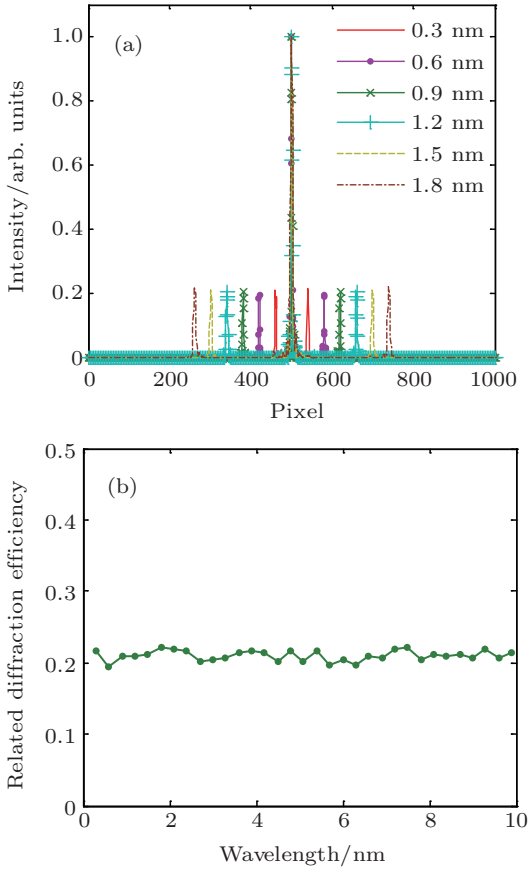


Fig. 5. (color online) (a) 1D diffraction patterns for various wavelengths, and (b) variation of relative diffraction efficiency of the 1st order with wavelength.

results are shown in Fig. 5(a) (the intensities are normalized by 0th order's peak values for convenience). Figure 5(a) clearly shows that there is only one visible diffraction order for each wavelength besides the 0th order, and the position of the 1st order diffractions changes linearly with wavelength. Hence the spectrum measured by the QRSPS can get rid of the influence of higher-order diffractions.

It is also necessary to analyze the diffraction efficiency of the QRSPS. Figure 5(b) shows the variation of the 1st order relative diffraction efficiencies of the QRSPS with a wavelength in a range between 0.3 nm and 10.0 nm, where the 1st order relative diffraction efficiency is defined as the ratio of the 1st diffraction intensity to the 0th order diffraction intensity. It can be seen from the figure that the 1st order relative diffraction efficiency is around 21% in the wavelength region that we are interested in.

3.3. Influence of X-ray's penetration

In the preceding parts of this paper, we have assumed that substrate (gold foil) absorbs all X-rays incident on it. However, considering the strong penetrability of X-rays and the limited thickness of gold foil, part of the incident X-rays can pass through the gold foil. For example, about 33 percent of incident X-rays will pass through the gold foil when the wavelength $\lambda = 0.3$ nm and the thickness of gold foil $h = 500$ nm. This inevitably has some influences on the diffraction pattern of the QRSPS.

The complex wave-number of X-ray in metal is

$$k' = (1 - \delta + \mathrm{i}\beta)\omega/c = (1 - \delta + \mathrm{i}\beta)k, \tag{7}$$

where ω is the frequency of the X-ray, c is the velocity of wave in vacuum, and β and δ are optical constants of that metal material.

For a metal foil with a thickness of h, the transmittance function of X-ray is

$$t = \mathrm{e}^{-k\beta h}\mathrm{e}^{\mathrm{i}k(1-\delta)h}. \tag{8}$$

This indicates that the X-rays would be weakened and a constant phase shift would appear when X-rays have passed through the metal foil. The intensity of the QRSPS diffraction pattern would be enhanced or weakened, depending on the constant phase shift, while the diffraction pattern itself is similar to that in the case of no X-ray penetration.

The modified transmittance function of the QRSPS is

$$t'(x,y) = t(x,y) + [1 - t(x,y)]\,\mathrm{e}^{-k\beta h}\mathrm{e}^{-\mathrm{i}k\delta h}. \tag{9}$$

And we simulate the diffraction pattern of the QRSPS using this new transmittance function. In the simulation, $h = 500$ nm, $\lambda = 0.3$ nm, and the optical constants of gold are $\delta = 1.75 \times 10^{-4}$ and $\beta = 5.17 \times 10^{-5}$. The diffraction pattern is shown in Fig. 6(a). From the picture we can see that the diffraction pattern of the considered X-ray penetration is similar to that of no X-ray penetration. There are also nine light spots and no new light spot appears. The position of light spots does not change. But the intensities of light spots are enhanced when the thickness of gold foil is 500 nm and incident wavelength is 0.3 nm. This is more clear in Fig. 6(b), which shows the 1D diffractions of the QRSPS with and without considering the X-ray penetration. It is obvious that the two curves are almost the same except that the curve with considering the penetration is a little higher. In a word, the QRSPS would retain its characteristic of single order diffraction when the X-ray penetration is taken into account.

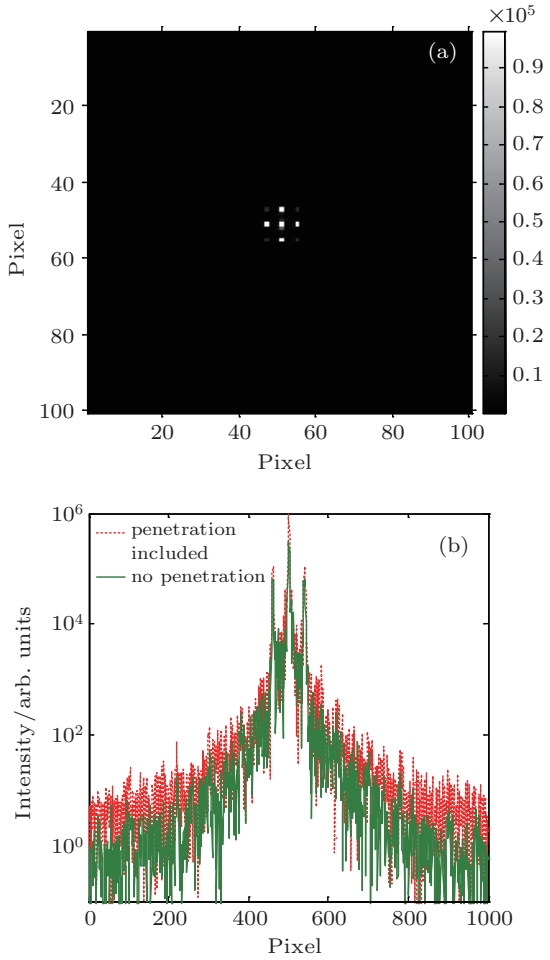


Fig. 6. (color online) (a) Diffraction pattern of the QRSPS with the X-ray penetration. (b) Comparison of the QRSPS 1D diffraction pattern between with and without the X-ray penetration.

4. Conclusion

In this paper, we proposed a new approach to the designing of the single order diffraction transmission grating in soft X-ray region, namely QRSPS. Its transmittance function across the grating bar is similar to that of STG. It suppresses higher-order diffraction effectively, even if the X-ray penetration is taken into account. The QRSPS may be a potential alternative option for soft X-ray spectra measurement.

References

[1] Hogan W J, Bangerter, Kulcinski R and G L 1992 *Phys. Today* **45** 42
[2] Lindl J 1995 *Phys. Plasmas* **2** 3933
[3] Lei Y H, Liu X, Guo J C, Zhao Z G and Niu H B 2011 *Chin. Phys. B* **20** 042901
[4] Wang J, Zhang H and Cheng X L 2013 *Chin. Phys. B* **22** 085201
[5] Attwood D 1999 *Soft X-ray and Extreme Ultraviolet Radiation, Principles and Applications* (Cambridge: Cambridge University Press) p. 55
[6] Born M and Wolf E 1980 *Principle of Optics* (London: Pergamon)
[7] Kipp L, Skibowski M, Johnson R L, Berndt R, Adelung R, Harm S and Seemann R 2001 *Nature* **414** 184
[8] Xie C Q, Zhu X L, Shi L N and Liu M 2010 *Opt. Lett.* **35** 1765
[9] Xie C Q, Zhu X L, Li H L, Shi L N and Wang Y H 2010 *Opt. Lett.* **35** 4048
[10] Xie C Q, Zhu X L, Li H L, Shi L N, Hua Y L and Liu M 2012 *Opt. Lett.* **37** 749
[11] Cao L F, Förster E, Fuhrmann A, Wang C K, Kuang L Y, Liu S Y and Ding Y K 2007 *Appl. Phys. Lett.* **90** 053501
[12] Wang C K, Kuang L Y, Wang Z B, Liu S Y, Ding Y K, Cao L F, Foerster E, Wang D Q, Xie C Q and Ye T C 2007 *Rev. Sci. Instrum.* **78** 053503
[13] Wang C K, Kuang L Y, Wang Z B, Cao L F, Liu S Y, Ding Y K, Wang D Q, Xie C Q, Ye T C and Hu G Y 2008 *Rev. Sci. Instrum.* **79** 123502
[14] Kuang L Y, Wang C K, Wang Z B, Cao L F, Zhu X L, Xie C Q, Liu S Y and Ding Y K 2010 *Rev. Sci. Instrum.* **81** 073508
[15] Kuang L Y, Cao L F, Zhu X L, Wu S C, Wang Z B, Wang C K, Liu S Y, Jiang S E, Yang J M, Ding Y K, Xie C Q and Zheng J 2011 *Opt. Lett.* **30** 3954
[16] Weng Y C, Kuang L Y, Gao N, Cao L F, Zhu X L, Wang X H and Xie C Q 2012 *Acta Phys. Sin.* **61** 154203 (in Chinese)
[17] Zang H P, Cao L F, Wang C K, Jiang G, Wei L, Fan W, Zhou W M and Gu Y Q 2011 *Acta Phys. Sin.* **60** 034215 (in Chinese)
[18] Zang H P, Wang C K, Gao Y L, Zhou W M, Kuang L Y, Wei L, Fan W, Zhang W H, Zhao Z Q, Cao L F, Gu Y Q, Zhang B H, Jiang G, Zhu X L, Xie C Q, Zhao Y D and Cui M Q 2012 *Appl. Phys. Lett.* **100** 111904
[19] Wei L, Cao L F, Fan W, Zang H P, Gao Y L, Zhu X L, Xie C Q, Gu Y Q, Zhang B H and Wang X F 2011 *High Power Laser and Particle Beams* **23** 387
[20] Gao Y L, Cao L F, Zhou W M, Wei L, Zang H P, Gu Y Q and Zhang B H 2011 *High Power Laser and Particle Beams* **23** 1523
[21] Gao Y L, Zhou W M, Wei L, Cao L F, Zhu X L, Zhao Z Q, Gu Y Q, Zhang B H and Xie C Q 2012 *Laser Particle Beams* **30** 313